
Article:
Wang, Xiuyi, Krieger-Redwood, Katya Melanie, Zhang, Meichao et al. (2022) Physical distance to sensory-motor landmarks predicts language function. Cerebral Cortex. bhac344. ISSN: 1460-2199

https://doi.org/10.1093/cercor/bhac344

OXFORD

Cerebral Cortex, 2022, 1–14
https://doi.org/10.1093/cercor/bhac344
Original Article

Physical distance to sensory-motor landmarks predicts language function

Xiuyi Wang[1,2,*], Katya Krieger-Redwood[2], Meichao Zhang[2], Zaixu Cui[3], Xiaokang Wang[4], Theodoros Karapanagiotidis[2], Yi Du[1,3,5,6], Robert Leech[7], Boris C. Bernhardt[8], Daniel S. Margulies[9,10], Jonathan Smallwood[11], Elizabeth Jefferies[2]

[1]CAS Key Laboratory of Behavioral Science, Institute of Psychology, Chinese Academy of Sciences, Beijing, 100101, China,
[2]Department of Psychology, University of York, Heslington, York YO10 5DD, UK,
[3]Chinese Institute for Brain Research, Beijing 102206, China,
[4]Department of Biomedical Engineering, University of California, Davis, CA 95616, USA,
[5]CAS Center for Excellence in Brain Science and Intelligence Technology, Shanghai 200031, China,
[6]Department of Psychology, University of Chinese Academy of Sciences, Beijing 100049, China,
[7]Centre for Neuroimaging Science, Kings College London, London, UK,
[8]McConnell Brain Imaging Centre, McGill University, Montreal, Quebec, Canada,
[9]Integrative Neuroscience and Cognition Center (UMR 8002), Centre National de la Recherche Scientifique (CNRS) and Université de Paris, Paris, France,
[10]Wellcome Centre for Integrative Neuroimaging, Nuffield Department of Clinical Neurosciences, University of Oxford, Oxford, UK,
[11]Department of Psychology, Queen's University, Kingston, Ontario, Canada

*Corresponding author: Email: wangxiuyi@psych.ac.cn

Auditory language comprehension recruits cortical regions that are both close to sensory-motor landmarks (supporting auditory and motor features) and far from these landmarks (supporting word meaning). We investigated whether the responsiveness of these regions in task-based functional MRI is related to individual differences in their physical distance to primary sensorimotor landmarks. Parcels in the auditory network, that were equally responsive across story and math tasks, showed stronger activation in individuals who had less distance between these parcels and transverse temporal sulcus, in line with the predictions of the "tethering hypothesis," which suggests that greater proximity to input regions might increase the fidelity of sensory processing. Conversely, language and default mode parcels, which were more active for the story task, showed positive correlations between individual differences in activation and sensory-motor distance from primary sensory-motor landmarks, consistent with the view that physical separation from sensory-motor inputs supports aspects of cognition that draw on semantic memory. These results demonstrate that distance from sensorimotor regions provides an organizing principle of functional differentiation within the cortex. The relationship between activation and geodesic distance to sensory-motor landmarks is in opposite directions for cortical regions that are proximal to the heteromodal (DMN and language network) and unimodal ends of the principal gradient of intrinsic connectivity.

Key words: default mode network; geodesic distance; gradient; language.

Introduction

A central question in cognitive neuroscience concerns how different functions emerge from the topography of the cortex (Huntenburg et al. 2018). In sensory-motor regions, functional responses are dominated by one modality—and since adjacent areas of cortex tend to have similar functions, physical proximity to visual, auditory or somatomotor regions is assumed to "tether" functional specificity to these unimodal processes (Jones and Powell 1970; Felleman and Van Essen 1991; Price et al. 2005; Chaudhuri et al. 2015; Jasmin et al. 2019). In contrast, regions that fall at a distance from sensory-motor systems along the cortical mantle, such as the default mode network (DMN), show more heteromodal and abstract responses, reflecting their untethered nature (Buckner and Krienen 2013; Mesulam 1998; Andrews-Hanna et al. 2010).

These contrasting functional responses are thought to reflect opposite ends of a functional gradient capturing the topographic transition from concrete/unimodal to abstract/heteromodal cortex (Mesulam 1998; Margulies et al. 2016; Buckner and DiNicola 2019; Buckner and Margulies 2019; Smallwood et al. 2021). Examples of this topography are found in different brain regions (Wang et al. 2020a; Bi 2021; Shaw et al. 2021; Muret et al. 2022). For example, neural representations elicited by visual inputs gradually vary from low-level visual features in primary visual cortex to more categorical and heteromodal responses further away (Felleman and Van Essen 1991; Chaudhuri et al. 2015; Chiou et al. 2018; Connolly et al. 2018; Wang et al. 2020a). Similarly, auditory cortex shows progressive selectivity for more complex sound types, with neural responses within primary auditory cortex tuned to simple features such as pure tones, and higher-order auditory areas such as superior temporal gyrus showing stronger responses to speech and music (Davis and Johnsrude 2003; Price et al. 2005; Chevillet et al. 2011; Hamilton et al. 2021). Auditory and visual processing streams are assumed to converge in ventral anterior temporal cortex, a heteromodal semantic hub (Lambon Ralph et al. 2017), with sites further away from this hub progressively more tied to a specific input modality (Visser et al. 2012; Irish et al. 2014; Coutanche and Thompson-Schill 2015; Hoffman et al. 2015; Humphreys et al. 2015). A similar gradient of abstraction has been proposed in frontal cortex

Received: May 10, 2022. **Revised:** August 1, 2022. **Accepted:** August 2, 2022

(Badre et al. 2009; Badre and Nee 2018; Wen et al. 2020): rostral frontal areas that are further from motor cortex support more abstract forms of control (Koechlin et al. 2003; Badre and D'Esposito 2007).

In this way, contemporary cognitive neuroscience argues that functional gradients provide an organizing principle to explain how both concrete and abstract processes arise within the cortex (Mesulam 1998; Plaut 2002; Margulies et al. 2016; Huntenburg et al. 2018). Consistent with this view, the principal gradient of intrinsic connectivity (i.e. the spatial component that explains the most variance in whole-brain patterns of brain activity) captures an orderly sequence of networks along the cortical surface in multiple cortical zones—with each region showing predictable transitions from primary sensory-motor systems, through attention networks to frontoparietal control and default mode networks (Margulies et al. 2016; Wang et al. 2020b). Crucially for the current study, the principal connectivity gradient is spatially correlated with physical distance from primary systems, capturing the spatial segregation of DMN from sensory and motor cortex (Margulies et al. 2016). This association suggests that two opposing functional relationships with distance might emerge in individual differences analyses: in brain regions that lie close to sensory-motor landmarks and consequently have a predominately sensory or motor function, individuals who show greater proximity to sensory-motor landmarks for a particular brain region might also show a stronger functional response to relevant inputs or outputs in that region. In contrast, for regions that are further away from sensory-motor landmarks and more engaged by abstract or memory-based aspects of tasks, greater distance should strengthen the functional response to relevant tasks, since separation from sensory-motor codes is thought to be required for these aspects of cognition (Margulies et al. 2016; Smallwood et al. 2021).

Our study tested these hypotheses about the relationship between physical distance from sensorimotor landmarks and functional responses during speech comprehension. Auditory language processing involves both sensory-motor and abstract semantic processes—and opposing relationships with distance are expected within the brain regions that support these functions. Building on the work of Mesulam (1998) and others (Jones and Powell 1970; Felleman and Van Essen 1991; Hill et al. 2010; Buckner and Krienen 2013; Xu et al. 2020), sensorimotor systems at the bottom of the cortical hierarchy are assumed to support concrete mappings between neural function and behavior, facilitating simple stimulus–response contingencies important for auditory-motor transformations in language. Acoustic and phonological processes recruited during both story comprehension and math tasks may be strengthened by greater proximity to auditory or oral-motor landmarks. Consequently, we might expect that regions within the auditory network will show stronger activation in response to spoken language inputs in individuals with a smaller distance between the auditory network parcel and transverse temporal sulcus (which provides a structural landmark for primary auditory cortex). In contrast, regions that support semantic aspects of language and are more responsive to spoken stories than math problems may show stronger activation in individuals with a greater cortical distance between the language parcel and sensory-motor landmarks, since increased distance should allow these relatively "untethered" heteromodal regions to encode abstract, invariant features that relate to word meaning.

Materials and methods

Datasets

The main dataset consisted of 1039 healthy volunteers (483 males, 556 females), aged 22–37 years (mean = 28.74, SD = 3.69), from the Human Connectome Project (HCP) (Glasser et al. 2013). The image acquisition, image preprocessing, fMRI analysis and parcellation of the HCP dataset have been described previously (Glasser et al. 2016, 2013) and see Supplementary Materials for details. Informed consent was obtained and the study was approved by the Institutional Review Board of Washington University at St. Louis.

Since the HCP language tasks were auditorily presented, we reanalyzed another dataset of 31 healthy adults collected at the University of York, UK, to examine the extent to which each parcel responded to visual language and maths inputs (Wang et al. 2021). (see Supplementary Materials for the detailed information about participants, image acquisition, image pre-processing and fMRI analysis).

Task paradigms

In the current study, we analyzed data from the auditory language and math tasks in the HCP dataset. The following task details are adapted from Barch et al. (2013). We also analyzed data from visually presented semantic, math, and spatial working memory tasks from a dataset collected at the University of York, and provide details about these tasks adapted from Fedorenko et al. (2011) and Wang et al. (2021). The York datasets help to confirm whether parcels showing an association between distance to sensory-motor cortex and activation are heteromodal or unimodal in their response, since we expect larger distances to be associated with greater activation for heteromodal regions, and smaller distances to be associated with greater activation for unimodal regions.

Language task from the HCP dataset

The task from Binder et al. (2011) consisted of two runs that each interleaved 4 blocks of a story task and 4 blocks of a math task. Each block was introduced with an auditory cue word, "story" or "math," presented 3 s prior to the beginning of the block. A response period of 2 s was provided after each story or math question. The lengths of the blocks varied (average of approximately 30 s), but the task was designed so that the math task blocks matched the length of the story task blocks, with some additional math trials at the end of the task to complete the 3.8-minute run as needed.

In story blocks, participants were presented with brief auditory stories (5–9 sentences) adapted from Aesop's fables, followed by a 2-alternative forced-choice question about the topic of the story. The example provided in Binder et al. (2011) is "After a story about an eagle that saves a man who had done him a favor, participants were asked, 'Was that about revenge or reciprocity?'" The probe questions were designed to be difficult so that participants attended closely to the stories. Multiple levels of difficulty of the story condition were created, defined by the vocabulary level of the story materials and the relative similarity of meaning of the response choices, so that the difficulty of the task could be adjusted based on ongoing performance. A training session outside the scanner was used to find an approximate level of difficulty for each participant. Further adjustment occurred automatically during scanning using a staircase method. The level increased in difficulty after 6 consecutive correct responses and decreased in difficulty after any incorrect response. The level at the start of each run was set to the level attained at the end of the preceding run. The mean difficulty level of the story task was

10.40 (SD = 1.48) and the range was 3.78 –12.57. Participants who were presented with more difficulty story materials had better performance on this task.

Math task from the HCP dataset

The math task was designed to provide a comparison with the story task that was attentionally demanding, similar in auditory and phonological input, and unlikely to generate activation of regions involved in semantic processing, though likely to engage number-related processing in the parietal cortex. The math task also presented trials auditorily and required participants to complete addition and subtraction problems. The trials were arithmetic operations (e.g. "fourteen plus twelve"), followed by "equals" and then two choices (e.g. "twenty-nine or twenty-six"). The participants pressed a button to select either the first or the second answer. The materials were generated using the same text-to-speech method used for the story task stimuli, with matched word and phoneme rate, speaking style, and prosodic features. The math task was adaptive to maintain a similar level of difficulty across the participants. The mean difficulty level of the math task was 2.56 and the range was small across participants (range was 1.14 – 3.86, SD = 0.61).

Visually-presented semantic task from the York dataset

Participants read sentences and lists of pronounceable nonwords, followed by a probe recognition test (present/absent judgment about a single word or nonword). Sentences contrasted with nonwords reliably activate high-level semantic and language regions (Fedorenko et al. 2011). Each trial started with a 100-ms blank screen. Stimuli were presented at the center of the screen, one item at a time, at the rate of 450 ms per item. The sequence was followed by a probe word/nonword; participants had 2 s to decide whether this item had been presented in the sequence, giving a total trial duration of 7.5 s. Each run included 16 experimental blocks with 3 trials per block and 5 fixation blocks lasting for 14 s. Each run lasted a total of 430 s. The fixation blocks were used as the implicit baseline for the univariate analysis.

Visually presented math task from the York dataset

In this task, participants performed addition with smaller or larger numbers, giving rise to easy and hard conditions. Participants saw an arithmetic expression on the screen for 1.45 s and were then given two numbers as potential answers, for 1.45 s. Each trial ended with a blank screen lasting for 0.1 s. Each run consisted of 12 experimental blocks (with four trials per block) and four fixation blocks, resulting in a total time of 316 s. This task included two runs containing the two conditions, presented in a standard block design. Condition order was counterbalanced across runs, and run order was counterbalanced across participants for each task. The fixation blocks were used as the implicit baseline for the univariate analysis.

Spatial working memory task from the York dataset

Participants had to keep track of four or eight sequentially presented locations in a 3 × 4 grid, giving rise to easy and hard spatial working memory conditions (Fedorenko et al. 2011). Stimuli were presented at the center of the screen across four steps. Each of these steps lasted for 1 s and highlighted one location on the grid in the easy condition and two locations in the hard condition. This was followed by a decision phase, which showed two grids side by side. One grid contained the locations shown on the previous four steps, while the other contained one or two locations in the wrong place. Participants indicated their recognition of these locations in a two-alternative, forced-choice paradigm via a button press, and feedback was immediately provided. Each run consisted of 12 experimental blocks (6 blocks/condition and four trials in a 32 s block) and four fixation blocks (each 16 s long), resulting in a total time of 448 s. This task included two runs containing the two conditions, in a standard block design. Condition order was counterbalanced across runs, and run order was counterbalanced across participants for each task. The fixation blocks were used as the implicit baseline for the univariate analysis.

HCP multi-modal parcellation and areal classifier

We used the HCP multi-modal parcellation map 1.0 (Glasser et al. 2016) in this study. This parcellation map was first created using a semi-automated approach utilizing the group average maps across multiple modalities. Combining multiple properties provides complementary as well as confirmatory information, as different properties distinguish different sets of areal boundaries, and more confidence can be placed in boundaries that are consistent across modalities. Glasser et al. (2016) analyzed four properties (i.e. cortical architecture, function, connectivity and topography), across all of neocortex in both hemispheres. Architectural measures of relative cortical myelin content and cortical thickness were derived from T1-weighted (T1w) and T2-weighted (T2w) structural images. Cortical function was measured using task functional MRI contrasts from seven tasks. Resting-state functional MRI revealed functional connectivity of entire cortical areas plus topographic organization within some areas. For each modality, a dissimilarity metric was computed between neighboring feature profiles generated from segmented histological images and tested for statistically significant and large spikes in dissimilarity that indicate putative areal boundaries. For each modality, the first spatial derivative along the cortical surface was used to identify ridges, i.e. local regions showing relatively sudden change. Overlapping ridges across modalities were used to draw putative areal borders with manual initialization and algorithmic refinement. Glasser et al. (2016) combined fully automated algorithmic approaches with manual or partly automated neuroanatomical approaches in which neuroanatomists delineated areal borders, documented areal properties, and identified areas after consulting prior literature. For the initial parcellation, they adapted an observer-independent semi-automated neuroanatomical approach for generating post-mortem architectonic parcellations to non-invasive neuroimaging. They used an algorithm to delineate potential areal borders (transitions in two or more of the cortical properties described above), which two neuroanatomists then confirmed according to the literature. Finally, they used a fully automated algorithmic approach, training a machine-learning classifier to delineate and identify cortical areas in individual subjects based on multi-modal areal fingerprints, allowing the parcellation to be replicated in new subjects and studies. This process identified 180 parcels per hemisphere. Each parcel varied in size and shape based on alignment between functional and anatomical borders across multiple imaging modalities.

This multimodal approach that anchors surface-based registrations to other structural and functional characteristics of an individual has been shown to improve subject to subject registrations, and hence reduce inter-subject variability (Grayson and Fair 2017). In line with this, it has been shown that parcellated maps are highly stable across individual subjects: the mean pairwise Spearman rank correlation between subjects' individual maps was 0.94 for the T1w/T2w map (Burt et al. 2018). Therefore, we

registered the group-level parcellation to each individual based on the vertex information of each parcel.

Task fMRI analysis

Task fMRI analysis steps are detailed in Barch et al. (2013). Briefly, temporal autocorrelation was estimated using FSL's FILM on the surface. Activation estimates were computed for the pre-processed functional time series from each run using a general linear model (GLM) implemented in FSL's FILM (Woolrich et al. 2001). For the language task, two predictors were included in the language processing model—story and math. The story predictor covered the variable duration of a short story, question, and response period (~30 s). The math predictor covered the duration of a set of math questions designed to roughly match the duration of the story blocks. We computed three contrasts: story only, math only and the linear contrast of story versus math. After model estimation, beta-weight images for the period of interest (story only and math only), contrasting the relevant time points with the implicit baseline (i.e. the fixation periods), was used to capture the relevant pattern of activation for each task.

All regressors were convolved with a canonical hemodynamic response function and its temporal derivative. The time series and the GLM design were temporally filtered with a Gaussian-weighted linear high pass filter with a cut off of 200 s. Finally, the time series was pre-whitened within FILM to correct for autocorrelations in the fMRI data. Surface-based autocorrelation estimate smoothing was incorporated into FSL's FILM at a sigma of 5 mm. Fixed-effects analyses were conducted using FSL's FEAT to estimate the average effects across runs within each subject. For further analysis of effect sizes, beta "cope" maps were generated using custom-built MATLAB scripts after moving the data from the CIFTI file format to the MATLAB workspace and after correction of the intensity bias field with an improved method (Glasser et al. 2016). Activation estimates on cortical surface vertices were averaged across vertices that shared the same areal label in a given subject.

To reveal the parcels showing stronger activation when listening to the story, we extracted the beta value of each parcel of each participant in the story condition and then conducted one sample t tests to test whether the beta values of each parcel were different from zero. Since all parcels were included, we conducted FDR correction at $P = 0.0001$ to control for multiple comparisons (Benjamini and Hochberg 1995). To identify parcels showing activation in the math task, we performed the same analysis using beta values for the math condition. Lastly, we used the same approach to identify parcels showing differential activation for story versus math tasks, using the beta value for this task contrast. All the results are visualized on the "very_inflated" surface to enable visibility within sulci using Connectome Workbench.

The global minimum geodesic distance to each landmark

DMN regions at the end of the principal gradient of intrinsic connectivity, associated with memory and aspects of cognition that are decoupled from the external world, have been shown to have the greatest geodesic distance along the cortical surface from primary sensory-motor regions (Margulies et al. 2016). This observation suggests that the function of regions might be influenced by their physical proximity to structural landmarks corresponding to primary sensory-motor regions. To investigate this possibility, we calculated the geodesic distance between each parcel and key landmarks associated with primary visual, auditory and somatomotor cortex. We used these values to identify the minimum geodesic distance to primary sensory-motor regions for each parcel. Three landmarks were used: central sulcus, which is the topographical landmark corresponding to primary somatosensory/motor cortex; temporal transverse sulcus, which provides a landmark for primary auditory cortex; and calcarine sulcus, marking the location of primary visual cortex. Since cortical folding patterns vary across participants, and individual variability in cortical folding increases with cortical surface area (Van Essen et al. 2019), both the shapes of these landmarks and the number of vertices within each landmark might show individual variability. We used participant-specific landmark label files to localize the participant-specific vertices belonging to each landmark.

The participant-specific landmarks were defined using FreeSurfer. First, FreeSurfer automatically reconstructs surface mesh representations of the cortex from individual subjects' T1 images. The cortical surface mesh is inflated into a sphere and registered to a common spherical coordinate system that aligns the cortical folding patterns across subjects (Dale et al. 1999; Fischl et al. 1999). The outcome of this procedure is a nonlinear mapping between the subject's native T1 space and fsaverage surface space. Second, the recon-all procedure generates corresponding surface parcellations of 74 sulci and gyri for each subject (lh.aparc.a2009s.annot and rh.aparc.a2009s.annot), which is the anatomical segmentation (Fischl et al. 2004; Desikan et al. 2006; Destrieux et al. 2010). FreeSurfer assigns these labels based on probabilistic information estimated from a manually labeled training set (Destrieux atlas) and geometric information derived from the cortical model of the subject. Then we resampled the individual surface from fsaverage space into fs_LR ~32 k space. After that, we extracted all the vertices belong to calcarine sulcus, central sulcus and transverse sulcus, respectively, for each individual. The use of individual-specific landmarks improved the precision of our study.

Geodesic distance along the "midthickness" of the cortical surface (halfway between the pial and white matter) was calculated using the Connectome Workbench software with an algorithm that measures the shortest path between two vertices on a triangular surface mesh (Mitchell et al. 1987; O'Rourke 1999). This method returns distance values that are independent of mesh density. Geodesic distance was extracted from surface geometry (GIFTI) files, following surface-based registration (Robinson et al. 2014). To ensure that the shortest paths would only pass through the cortex, vertices representing the medial wall were removed from the triangular mesh in this analysis.

We calculated the minimum geodesic distance between each vertex and each landmark. Specifically, when the landmark was central sulcus, we calculated the geodesic distance between vertex i outside central sulcus and each vertex within the central sulcus (defined for each individual; see above). Then we found vertex j within the central sulcus that was closest to vertex i, and extracted this value as the minimum geodesic distance between vertex i and this landmark. To compute the minimum geodesic distance between parcel k and the central sulcus, we computed the average minimum distance across all the grayordinate vertices in parcel k to the vertices within the central sulcus. We used the same procedure to calculate minimum geodesic distance between each parcel and all three sensory-motor landmarks (calcarine and temporal transverse sulci as well as central sulcus). From these three minimum geodesic distances identified between parcel k and sensory-motor landmarks, we then selected

the lowest distance value (i.e. the landmark that was closest to parcel *k*) to define the global minimum distance to sensory-motor regions for parcel *k*.

Whole-brain functional connectivity gradients

To examine the relationship between the principal gradient of intrinsic connectivity and global minimum distance metric described above, we performed dimension reduction analysis on resting state data. We identified the principal dimension of the resting state functional connectivity matrix across 360 parcels to obtain the principal gradient. First, the functional time-series from 360 regions of interest (ROIs) was extracted for each individual using the Glasser parcellation (Glasser et al. 2016). Pearson correlation was calculated to construct a 360×360 connectivity matrix for each participant. These individual connectivity matrices were then averaged to calculate a group-averaged connectivity matrix. The Brainspace Toolbox (Vos de Wael et al. 2020) was used to extract ten group-level gradients from the group-averaged connectivity matrix (dimension reduction technique = Laplacian eigenmaps, kernel = Pearson, sparsity = 0.9), in line with previous studies (Mckeown et al. 2020; Wang et al. 2020b).

The correlation between principal connectivity gradient and global minimum distance

We firstly calculated the correlation between gradient values and global minimum distance of the 180 parcels in the left hemisphere. Given the spatial autocorrelation present in both the principal connectivity gradient and global minimum distance maps, we created a null distribution using spin permutation implemented in BrainSMASH (Burt et al. 2020). This approach simulates brain maps, constrained by empirical data, that preserve the spatial autocorrelation of cortical parcellated brain maps. We then compared the observed correlation value with the null distribution for left hemisphere to examine whether the correlation between gradient values and global minimum distance of parcels in the left hemisphere was significantly greater than expected from spatial autocorrelation alone. Similarly, we examined the correlation between gradient values and global minimum distance of the 180 parcels in the right hemisphere using the same methods. This analysis was performed for the two hemispheres separately because the geodesic distance between parcels was used to generate the spatial-autocorrelation-preserving surrogate maps when creating the null distribution, and we could only measure geodesic distance between parcels within a hemisphere, because the left and right hemisphere surface maps were not on the same mesh.

The correlation between activation strength and global minimum distance

To investigate whether the functional response of parcels to the language and math tasks was related to their minimum distance to primary sensory-motor cortex, we calculated the correlation between activation strength and global minimum distance to primary landmarks for each parcel. We performed this analysis both for parcels that showed (i) significant activation in both the story and math conditions (i.e. auditory-verbal regions) and (ii) greater activation for the story than the math task (i.e. semantic-language regions). For each of these parcels, we extracted the beta values for the relevant contrast (the sum of activation in the story and math conditions, and story versus math activation, respectively). Then we calculated the correlation between these beta values for each participant and the minimum distance for the relevant parcel to the closest sensory-motor landmark in each individual. We imputed outliers above 3 SD from the mean with this cut-off value to reduce the effect of extreme values on the correlation coefficients. To test for statistical significance, we permutated the global minimum distance values across participants 1000 times; we then calculated the correlation between activation strength and permutated global minimum distance to build a null distribution for each parcel. Since we included multiple parcels, we used the permutation-based maximum r and minimum r values in the null distribution for each parcel to control the family-wise error (FWE) rate ($P = 0.001$, FWE-corrected). To evaluate significance, if the observed *r* values were positive, we counted the fraction of times of r values in the maximum null distribution were greater than the observed "true" *r* values; if the observed *r* values were negative, we counted the fraction of times of r values in the minimum null distribution were less than the observed "true" *r* values. The FWE correction was controlled for the two analyses, respectively.

Control analysis of parcel size

Given that parcel size (i.e. surface area) was correlated with the distance between parcels (see Results), we conducted control analyses examining the relationship between parcel surface area for each individual and task activation. The surface area of each parcel was calculated using surface geometry (GIFTI) files, using the Connectome Workbench software. Each vertex was assigned one third of the triangular area it defined. Surface area values were averaged across vertices that shared the same areal label in a given participant to get the parcel-based surface area.

The correlation between task activation and global minimum distance to sensory-motor landmarks varies along the principal gradient of intrinsic connectivity

This analysis investigated whether the relationship between task activation and global minimum distance to sensory-motor landmarks differs for parcels situated towards the DMN and sensory-motor ends of the principal connectivity gradient. We might expect parcels close to sensory-motor landmarks to show more activation across tasks when minimum distance is lower (i.e. negative correlations between activation and distance), since this pattern is expected to be associated with more functional access to sensory-motor information. Conversely, we might expect parcels at a greater distance from sensory-motor areas to show more activation when minimum distance is higher (i.e. positive correlations between activation and distance), since this pattern might strengthen abstract aspects of cognition, supporting the memory retrieval and cognitive control elements of the language and math tasks. To test this hypothesis, we assessed the relationship between the average principal gradient value for each parcel and the previously-computed correlation values between activation strength in the story and math conditions and global minimum distance. We specifically examined the parcels showing activation in both the story and math conditions, since these were distributed along the length of the principal gradient. We extracted r values reflecting the correlation between global minimum distance and the summed activation in the story and math condition for each parcel and transformed them to Fisher z values. We calculated the correlation between the Fisher z values and the values for these parcels on the principal gradient of intrinsic connectivity.

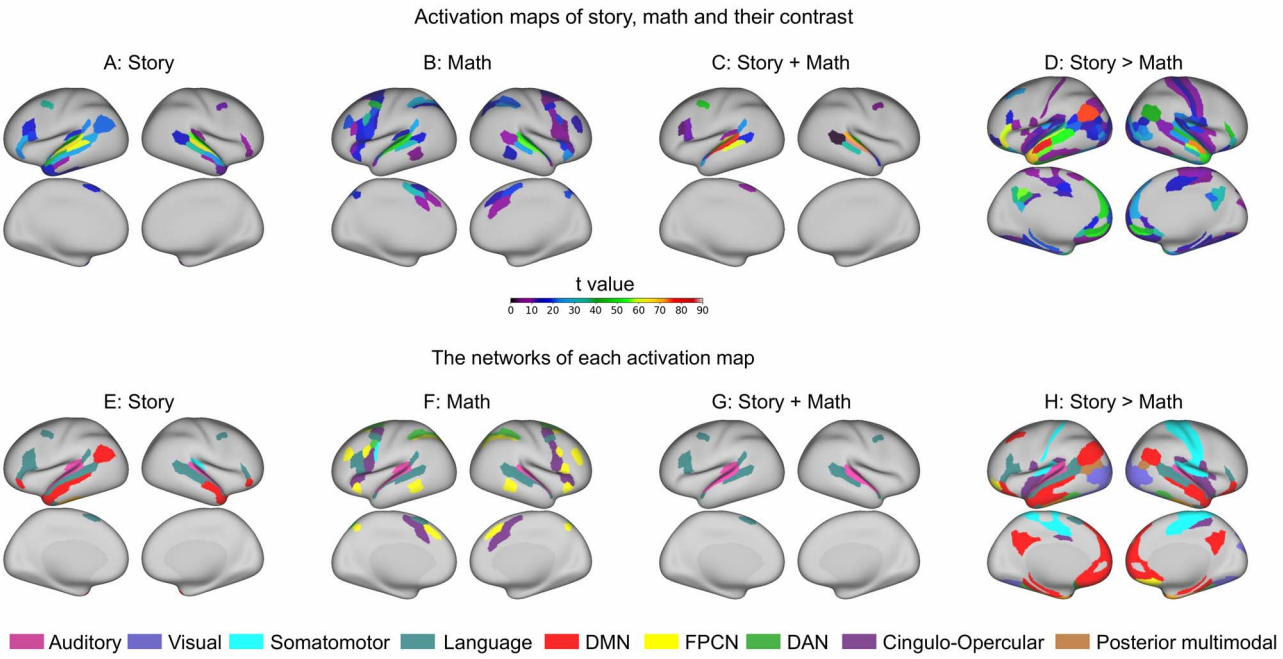

Fig. 1. Parcels that are activated in story and math tasks and the networks they belong to. A, B—Parcels that show stronger activation in the story and math conditions relative to implicit baseline, respectively ($P = 0.0001$, FDR corrected). C—The overlapping regions between A and B activated by both tasks. D—Parcels that show stronger activation in the story condition relative to the maths condition. E, F, G, and H show the networks that the parcels in A, B, C, and D belong to (Ji et al. 2019).

Code

The code for this study is available at https://github.com/Xiuyi-Wang/Language_Distance_Project.

Results

Regions activated by auditory story and math tasks

We identified regions involved in auditory story comprehension and math tasks using the Glasser parcellation (Glasser et al. 2016). We extracted the beta value of each parcel in these task conditions and tested whether they were significantly activated (i.e. above zero). We then identified the network that each parcel belonged to (Ji et al. 2019). Parcels in the auditory, language network and DMN were activated for the story task (Fig. 1A and E). For the math task, activated parcels were identified in the auditory, language, somatomotor, cingulo-opercular, dorsal attention, and frontoparietal networks (Fig. 1B and F). Next, we identified parcels that were commonly activated across these two auditory tasks. The conjunction of these tasks highlighted parcels in the auditory and language networks (Fig. 1C and G). Finally, we considered parcels that showed stronger activation in the story than the math task. This identified parcels in visual, auditory, language and default mode networks (Fig. 1D and H). All P values are FDR corrected at $P < 0.0001$.

Global minimum distance to primary sensory-motor landmarks

A key aim of this study was to examine whether individual differences in activation within the parcels responding to the auditory-verbal tasks at the group level (identified in 3.1) were related to variation in distance from sensory-motor landmarks across individuals. The top panel of Fig. 2 shows the average minimum distance map for each sensory-motor landmark, with purple-blue regions highlighting parcels that are closer to these landmarks, and orange-red regions highlighting parcels that are further away on the cortical mantle. Fig. 2A–C show distance to the temporal transverse sulcus (marking the location of primary auditory cortex), the central sulcus (i.e. distance to primary motor cortex) and the calcarine sulcus (i.e. distance to primary visual cortex), respectively. These maps were combined in Fig. 2D to provide a group-level representation of global minimum distance from sensory-motor cortex: medial prefrontal cortex was maximally distant from all three of these landmarks, with relatively high global minimum distances also observed in posterior parietal cortex and ventrolateral temporal cortex (relative to the surrounding cortex).

The principal connectivity gradient correlates with global minimum distance

Previous work has suggested that global minimum distance to sensory-motor landmarks has functional significance. It has been found that global minimum distance from sensory-motor cortex was correlated with the principal gradient of intrinsic connectivity, which captures the separation between unimodal and transmodal regions (Margulies et al. 2016). Our next analysis therefore considered the relationship between global minimum distance and the principal component of intrinsic connectivity to verify this association between distance and functional connectivity. We computed the parcel-to-parcel intrinsic connectivity matrix for each participant and extracted dimensions of connectivity space at the group level. As expected, the dimension explaining the most variance corresponded to the principal gradient as described by Margulies et al. (2016): sensory-motor regions fell at one end of this dimension of connectivity (shown in purple-blue in Fig. 2E), while transmodal areas were located at the other (shown in red-orange in Fig. 2E). We also found significant correlations between the principal gradient of connectivity and global minimum

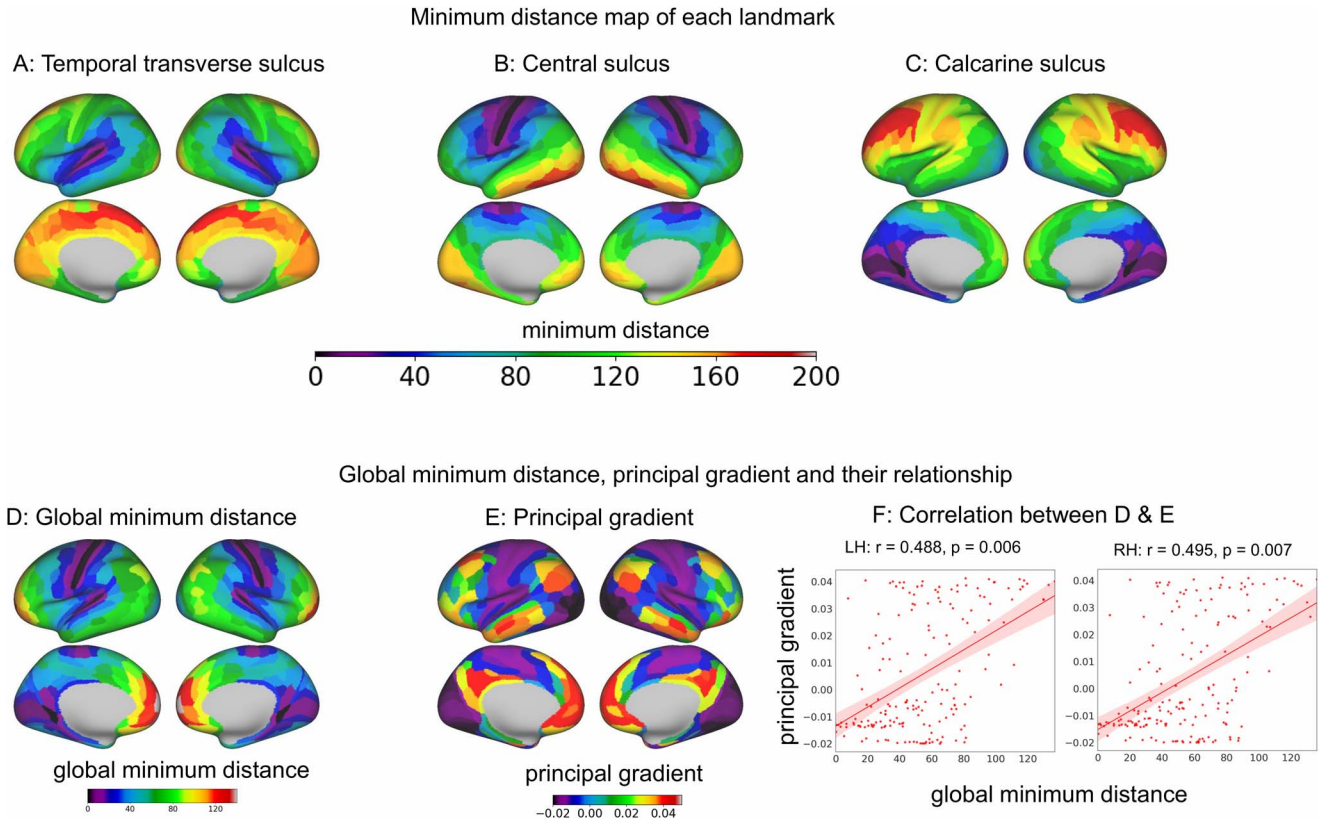

Fig. 2. The minimum geodesic distance between each parcel and each landmark and its relationship with the principal connectivity gradient. A, B, C—The minimum distance between each parcel and temporal transverse sulcus, central sulcus and calcarine sulcus, respectively. D—The global minimum geodesic distance between each parcel and the closet landmark. E—The principal connectivity gradient that explained the most variance in resting-state fMRI. F—The global minimum geodesic distance is significantly correlated with the principal connectivity gradient for each hemisphere (spin permutation corrected; LH = left hemisphere; RH = right hemisphere).

distance in both hemispheres, which could not be explained in terms of spatial autocorrelation (left hemisphere: $r = 0.488$, $P = 0.006$; right hemisphere: $r = 0.495$, $P = 0.007$; spin-permutation FWE corrected).

Auditory-verbal functional activation correlates with global minimum distance

Having established which parcels were reliably activated by these auditory-verbal tasks, we examined whether individual differences in the minimum distance of these parcels to sensory-motor landmarks were associated with variation in this functional activation. Correlation between task activation and distance along the cortical mantle would provide further support for the view that cortical distance provides an explanation for functional differentiation in sensory-motor and association cortex.

First, we examined parcels showing common responses across the language and math tasks. These parcels are expected to include both unimodal regions that respond to auditory inputs and heteromodal language regions that support lexical access across these tasks. We extracted the beta value for these parcels in both the story and math conditions and then summed them; we then calculated the correlation between the summed beta value and the global minimum distance across participants for each parcel. Regions in the auditory network—in bilateral primary auditory cortex and right TA2—showed a negative correlation between the summed beta value of the story and math conditions and global minimum distance (Fig. 3A; $r = -0.134$, $P < 0.001$; $r = -0.174$, $P < 0.001$; $r = -0.109$, $P = 0.005$, FWE corrected): participants who showed stronger activation across these tasks tended to have shorter distances between these parcels and temporal transverse sulcus (Figs. 3B–D). Conversely, regions in the language network, in bilateral 55b, showed a positive correlation between the summed beta value of the story and math conditions and global minimum distance (Fig. 3A; $r = 0.131$, $P < 0.001$; $r = 0.109$, $P = 0.005$, FWE corrected): when this region was more distant from central sulcus, participants tended to show stronger auditory-verbal activation (Fig. 3E and F). Supplementary analyses confirmed that these positive and negative correlations with between activation and physical distance were also significant for each task separately (except for right 55b in the math task) (section 3.1 in Supplementary Materials).

To verify the functional specialization of these parcels, we used a second dataset that examined activation for *visual* semantic, math and spatial working memory tasks. We expect regions showing a negative correlation between sensory-motor distance and functional activation in the HCP data to activate specifically to auditory inputs, since shorter cortical distances should correspond to greater tethering to sensory inputs. Right primary auditory cortex and right TA2 in the auditory network showed significant deactivation for visually presented word, pseudoword, math and spatial working memory tasks versus rest (FDR corrected $P < 0.05$). Left A1 showed significant deactivation for the visually-presented math task (FDR corrected $P = 0.003$) and no response in the other tasks ($P > 0.05$) (see Supplementary Tables S1, S2 and S3). These parcels, which all showed negative distance-activation relationships, therefore showed the expected pattern of selective activation to auditory materials.

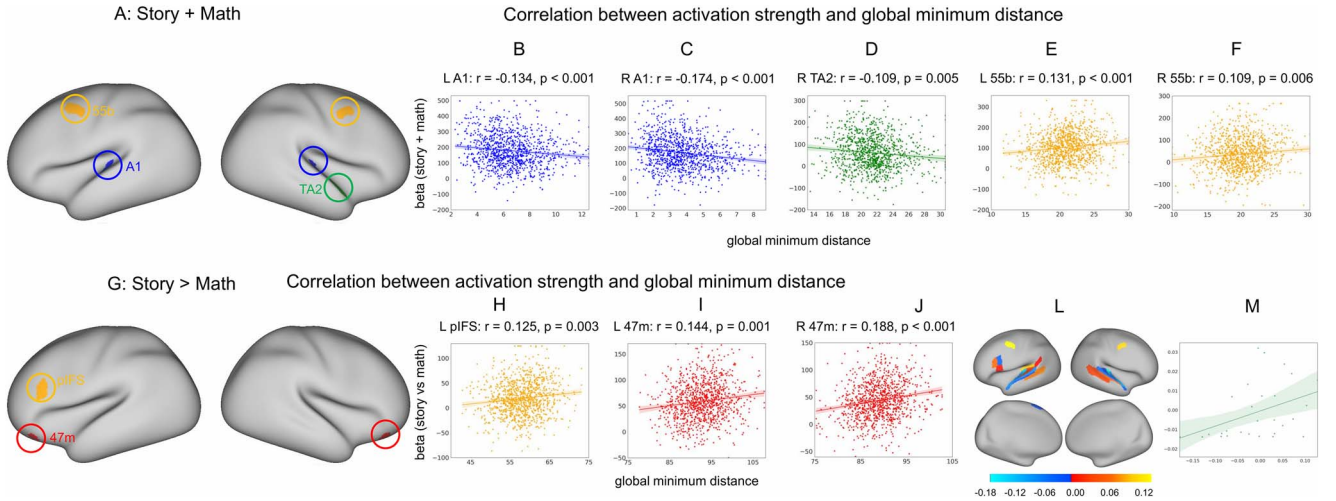

Fig. 3. Upper panel: A—The parcels whose summed activation strength in the story and math condition was correlated with global minimum geodesic distance. Three parcels in the auditory network (bilateral primary auditory cortex, A1, blue color and right TA2, green color) showed a negative correlation. Bilateral 55b (orange color, within the language network) showed a positive correlation. B, C, D, E, and F—The scatter plot for each parcel showing the correlation between the sum of activation strength in the story and math condition and global minimum distance. Each dot represents the data of one participant. B—left A1. C—right A1. D—right area TA2. E—left 55b. F—right 55b. Bottom panel: G—The parcels where activation strength in the contrast story > math was positively correlated with global minimum geodesic distance. H, I, J—These parcels were located in left posterior inferior frontal sulcus (orange color, within the language network) and bilateral 47 m (red color, within the default mode network). The relationship between activation in the story and math condition and global minimum distance varies along the principal connectivity gradient. L—Parcels that show stronger activation relation to the implicit baseline in the auditory story and math task. The colour represents the correlation values (Fisher z) between activation across auditory tasks and global minimum distance for each parcel. M—Principal gradient values were associated with the relationship between activation and distance for parcels responding across the story and math conditions, which extended from unimodal to association cortex ($r = 0.402$, $P = 0.033$, each dot represents a parcel in L).

Area 55b, in contrast, showed more activation in participants for whom the distance from sensory-motor cortex was greater. This is the pattern expected for regions that support more abstract and heteromodal aspects of language. Since bilateral 55b in the language network showed activation in both the story and math tasks and no difference between these conditions in the HCP dataset, this region might be involved in lexical-phonological as opposed to conceptual aspects of language processing. To test this hypothesis, we examined whether this region responded to visually-presented words and non-words in the York dataset. Bilateral 55b showed activation over rest for visually presented words (left 55b: $t = 12.296$, $P = 2.51e\text{-}12$; right 55b: $t = 2.649$, $P = 0.026$) and no activation for the spatial working memory task ($P > 0.05$). Left 55b but not right 55b showed activation over rest for visually presented nonwords ($t = 4.646$, $P = 0.0002$) and math problems ($t = 4.656$, $P = 0.001$). These findings are consistent with a role in heteromodal aspects of language processing. All *P*-values are FDR-corrected.

Next, we examined parcels that showed greater activation in the story than the math task, indexing a semantic response, which should be found within heteromodal cortex. We extracted the beta values for the story versus math contrast and examined the correlation with individual differences in global minimum distance. We found activation strength positively correlated with global minimum distance in three frontal parcels within the language network and DMN: left posterior inferior frontal sulcus ($r = 0.125$, $P = 0.003$) and bilateral 47 m (left 47 m, $r = 0.144$, $P < 0.0001$; right 47 m, $r = 0.188$, $P < 0.0001$; all results FWE corrected; Fig. 3G–J). Participants who showed a stronger response to the story than the math task in these parcels also tended to have greater geodesic distance between these parcels and primary sensory-motor landmarks.

To examine the extent to which these three parcels showing greater activation for the story task with greater distance from sensory-motor landmarks supported semantic processing across modalities, we assessed their responses to visually presented words and nonwords, math problems and spatial working memory using the York dataset. Left posterior inferior frontal sulcus in the language network responded to visual words and nonwords, with a stronger response for meaningful words ($t = 4.08$, $P < 0.002$). This parcel therefore showed a heteromodal semantic response across both auditorily and visually mediated language tasks. The parcel also showed a stronger response to more demanding math ($t = 7.009$, $P < 0.0001$) and spatial working memory ($t = 3.909$, $P < 0.001$) tasks, suggesting its contributions to cognition are not exclusively semantic. Bilateral 47 m in DMN showed significant deactivation for the math and spatial working memory tasks, with stronger deactivation for harder math judgments (left 47 m: $t = -3.038$, $P = 0.009$; right 47 m: $t = -4.247$, $P = 0.001$, FDR-corrected). We did not observe semantic activation in the visual word task, potentially because the semantic demands in this task were much lower than for story comprehension (see Supplementary Tables S1, S2 and S3).

To investigate the functional significance of the parcels whose activation strength was correlated with global minimum distance, we examined the correlation between activation and behavioral performance. As shown in Supplementary Fig. S1 and S2, the activation strength of bilateral 55b in the story condition was positively correlated with the difficulty level of the story material, reflecting participants superior performance (left 55b, $r = 0.113$, $P < 0.0001$; right 55b, $r = 0.063$, $P = 0.041$; uncorrected *P*; Supplementary Fig. S1). Similarly, the activation strength of left posterior inferior frontal sulcus ($r = 0.067$, $P = 0.03$), left 47 m ($r = 0.166$, $P < 0.0001$) and right 47 m ($r = 0.098$, $P < 0.002$; uncorrected *P*; Supplementary Fig. S2) in the story versus math contrast was positively correlated with the difficulty level of the story material. Participants who showed more activation in these regions were presented with more difficult story materials, and showed better performance, but we cannot fully deconfound the influence of these factors. Nevertheless, we can exclude the

possibility that increased brain activity was associated with worse function.

The correlation between activation strength and surface area

The global minimum distance to sensory-motor landmarks was highly correlated with surface area for the majority of parcels showing a positive correlation between activation strength and global minimum distance (bilateral 55b: $r = 0.39$, $P < 0.0001$; bilateral primary auditory cortex: $r = 0.191$, $P < 0.0001$; right TA2: $r = 0.181$, $P < 0.0001$, left posterior IFS: $r = 0.142$, $P < 0.0001$; bilateral 47 m: $r = 0.087$, $P = 0.278$; FWE-corrected). Consequently, we asked to what extent the correlation between activation strength and global minimum distance might be driven by the surface area of these parcels. To address this question, we calculated the correlation between the activation strength and the surface area of these parcels. The summed activation in the story and math condition was not correlated with surface area in left primary auditory cortex ($r = 0.041$, $P = 0.182$), right primary auditory cortex ($r = -0.049$, $P = 0.114$) or right TA2 ($r = 0.0006$, $P = 0.285$; all P values are uncorrected). However, activation across the story and math conditions was positively correlated with surface area for two parcels, left 55b ($r = 0.265$, $P < 0.0001$) and right 55b ($r = 0.088$, $P = 0.004$; P values are uncorrected). This suggests that surface area in 55b might contribute to this parcel's functional relationship with distance.

Activation for the story versus math contrast was not correlated with surface area in left posterior inferior frontal sulcus ($r = -0.012$, $P = 0.697$) or right 47 m ($r = -0.044$, $P = 0.152$). The activation strength in left 47 m was negatively correlated with surface area ($r = -0.129$, $P < 0.0001$).

How does the association between global minimum distance and activation change along the principal gradient?

Given the analysis above yielded significant associations between cortical distance to sensory-motor landmarks and activation in only a small number of regions, we performed additional analyses to establish this relationship also holds across the brain more widely. Our hypothesis was that parcels close to primary landmarks should have negative correlations between activation and distance (i.e. show less activation when they are further away from sensory-motor landmarks), while parcels nearer transmodal cortex should have positive correlations (i.e. show more activation when they are further away). We identified parcels showing activation in both the story and math conditions, which were distributed along the whole length of principal gradient, irrespective of whether their activation was significantly correlated with geodesic distance ($n = 28$). We extracted the correlation values between activation across auditory tasks and global minimum distance for each parcel and transformed the r values to Fisher z values (Fig. 3L). We also extracted the principal gradient values of these parcels. Finally, we examined the association between these principal gradient values and the Fisher z transformed distance-activation correlations across parcels. We found the principal gradient was significantly correlated with the strength of the distance-activation relationship (Fig. 3M; $r = 0.402$, $P = 0.033$). This suggests that the relationship between the activation in the story and math conditions and global minimum distance changes along the principal connectivity gradient.

For completeness, we also examined the association between the principal gradient and the relationship between distance and activation for parcels showing a stronger response to the story than the math task. We assessed the link between the principal gradient value and the Fisher z transformed correlation between activation in the story versus math contrast and global minimum distance. We included all parcels showing stronger activation to stories than math problems. There was no correlation ($r = -0.048$, $P = 0.516$), which might reflect the relative absence of parcels identified by this contrast at the unimodal end of the gradient, and/or the absence of a correlation between activation and global minimum distance for the majority of parcels in this analysis (178 out of 182 parcels, $P > 0.05$).

Discussion

Our study set out to test the hypothesis that distance from sensorimotor regions provides an organizing principal of functional differentiation within the cortex. We investigated whether the functional response of regions involved in auditory language comprehension is related to their physical distance to primary sensorimotor regions and how this association with geodesic distance differs for regions situated towards the transmodal and unimodal ends of the principal gradient of intrinsic connectivity. We found that among regions that were strongly activated in both the story comprehension and math tasks, participants who showed stronger activation in three regions in the auditory network (bilateral primary auditory cortex and right TA2) tended to have shorter distances between these parcels and temporal transverse sulcus (corresponding to primary auditory cortex). In contrast, regions in the language network (bilateral 55b in frontal cortex) were more distant from central sulcus for participants showing stronger auditory-verbal activation. Regions in the language network and DMN also showed a stronger response to the story than the math task; among these parcels, three regions (left posterior inferior frontal sulcus and bilateral 47 m within anterior inferior frontal gyrus) had greater geodesic distance to primary sensory-motor landmarks for participants who showed a larger effect of this task contrast. These results demonstrate that the function of regions involved in auditory language processing is related to their physical distance to primary sensorimotor cortex and the relationship between activation and geodesic distance is in opposite directions for cortical regions proximal to association (DMN and language network) and unimodal ends of the principal gradient of intrinsic connectivity.

Language-responsive regions are situated along a gradient of networks extending from auditory and motor cortices to transmodal cortices supporting higher-level cognitive functions (Braga et al. 2020; Wang et al. 2020b). Auditory language comprehension involves diverse representations; including acoustic (spectrotemporal analysis), phonological (capturing sensory to articulatory links), lexical (i.e. the patterns of letters and sounds that capture words) and semantic information about word meaning (Binder and Desai 2011; Fedorenko et al. 2011; Albouy et al. 2020; Braga et al. 2020; Hamilton et al. 2021). These aspects of language are processed in different regions that lie at different distances along the unimodal-to-transmodal hierarchy captured by the principal gradient (Margulies et al. 2016). Acoustic representations of words are associated with temporal regions proximal to auditory cortex (Albouy et al. 2020; Hamilton et al. 2021), while more abstract codes corresponding to multimodal word forms and word meaning are located away from input regions, for example in inferior frontal gyrus, anterior temporal cortex and angular gyrus regions, overlapping with DMN (Bonner et al. 2013; Fedorenko et al. 2010; Humphreys et al. 2015; Zhao et al. 2017). These distinctions within language, relating to functional responses associated with the

processing of acoustic word forms and abstract meanings, are proposed to reflect the topographical organization of the brain (Mesulam 1998; Buckner and Krienen 2013; Braga et al. 2020; Smallwood et al. 2021).

The tethering hypothesis (Buckner and Krienen 2013), in line with the topological schema proposed by Mesulam (1998), anticipates that when regions are strongly associated with sensory and motor inputs, encoding of this information is less influenced by motivational, emotional and attentional modulations in transmodal regions that follow from the internal state and experience of the individual. Therefore, the fidelity of modality-specific encoding is protected. In line with this, we found that greater proximity of the temporal transverse sulcus to auditory network parcels facilitated acoustic-phonological processing. These parcels showed a selective response to auditory inputs, with no activation or significant deactivation in response to visually presented language and non-language tasks. In contrast, when transmodal regions are further away from sensory and motor systems, this increased cortical distance is thought to allow brain regions to operate in a manner that is not dominated by any specific sensory-motor modality, and that can reflect relevant information in memory even when this is at odds with the external environment (Murphy et al. 2018). This type of processing is thought to be critical for the semantic access necessary for story comprehension (Pylkkänen 2019). In line with this, we observed that three frontal regions in the language network and DMN showed greater activation in the auditory story than the math task (i.e. a stronger semantic response) when they were at a greater distance to sensory-motor landmarks. The increased activation might reflect either better performance or more challenging materials but not worse performance (i.e. compensatory increases in the BOLD response reflecting neurocognitive weakness) because participants with better performance were presented with more difficult materials in the scanner for the HCP tasks we analyzed. The left inferior frontal sulcus also showed stronger activation in response to visual words than pronounceable nonwords, suggesting a multimodal semantic response for this site. This is consistent with previous findings that this region showed stronger activation for words than nonwords no matter whether the stimuli were visually or auditorily presented, even when these modalities were compared using the same participants and same scanning protocols (Fedokenro et al. 2010). Furthermore, the language parcels defined in the HCP dataset (Barch et al. 2013) greatly overlapped with the language parcels defined in another independent dataset (Lipkin et al. 2022). Bilateral 47 m did not show stronger activation for written words versus nonwords, perhaps because the semantic demands in the visually-presented word task were much lower than for story comprehension. In addition, although the HCP and York datasets were scanned using different protocols, we used cutting-edge methods to improve cortical area localization and alignment across participants and datasets. We performed all the analysis on the surface to improve the alignment of areas across participants, since volume-based smoothing and registration substantially degrades localization compared with surface-based approaches (Coalson et al. 2018). The comparison between these datasets is therefore informative about the heteromodal versus unimodal tuning of each region, even though an ideal design would use the same scanning protocols and same materials in the same participants to establish how each parcel responds across modalities.

One outstanding question concerns the extent to which the association between cognitive function and global minimum distance to sensory-motor cortex is common or divergent across different regions of cortex that are proximal to different sensory-motor systems. Auditory and motor cortex are the most functionally relevant primary systems for language and, in this study, all of the parcels showing a negative association between distance and language activation were closest to auditory and motor landmarks. The functional relevance of auditory-motor transformations to language may explain why parcels proximal to visual cortex, and DMN regions not relevant to semantic cognition, did not show a functional relationship with distance. Although transmodal regions are widely distributed across the brain, each region within DMN is closer to particular unimodal features of experience than others, potentially giving rise to functional specialization within local gradients that are nevertheless still nested within the whole-brain principal gradient (Smallwood et al. 2021). For example, auditory cortex is notably closer to certain nodes of the DMN (including inferior frontal gyrus) than other primary systems and these regions are important for language processing in analyses of individual participants (Braga et al. 2020). This proximity to the auditory system might allow these DMN regions capitalize on the capacity for language processes to organize cognitive function.

In our analysis, a relatively small number of individual parcels showed significant correlations between activation strength and geodesic distance. Moreover, our relatively stringent approach to correcting for multiple comparisons may have given rise to Type 2 errors. Further research is needed to replicate the relevance of distance to function in the parcels we identified here and to establish whether the relationship between distance and activation is stronger in these specific parcels compared with other parcels in the same sensory and heteromodal networks. Given the sparse nature of the results, we also considered the relationship between activation in the story and math conditions and global minimum distance across all regions responsive across the language and math tasks. The relationship between activation and distance changed systematically along the principal connectivity gradient: parcels close to sensory-motor landmarks showed more activation across tasks when minimum distance was lower (i.e. more negative correlations between activation and distance), since this pattern is associated with more functional access to sensory-motor information. Conversely, parcels at a greater distance from sensory-motor areas showed more activation when global minimum distance was higher (i.e. stronger positive correlations between activation and distance); this pattern might strengthen abstract aspects of cognition, supporting memory retrieval and cognitive control elements of the language and math tasks.

In addition, the relationship between function and physical distance could not be explained by individual differences in surface area for all the identified regions except bilateral 55b. Bilateral 55b showed stronger activation in both the auditory story comprehension and math tasks relative to rest, with no difference between these conditions. The responsiveness of 55b to a wide range of language tasks, involving both spoken and written inputs, and math judgments as well as story comprehension, suggests that this region is not task or modality-specific (Du et al. 2014; Du et al. 2016; Dichter et al. 2018; Chang et al. 2020; Poologaindran et al. 2020; Sarubbo et al. 2020). It often shows stronger activation for words than pronounceable nonwords, suggesting this region might support high-level language processing (Fedokenro et al. 2010; Braga et al. 2020; Lipkin et al. 2022). It is not clear from this study how distance along the cortical mantle and surface area contribute to the functions of area 55b. A larger surface area might lead to more activation because when this region

is larger, motor language functions are better supported. Alternatively, greater distance from central sulcus might strengthen more abstract aspects of language processing, consistent with the heteromodal response of area 55b across diverse language tasks. Future research contrasting different kinds of language tasks—for example, promoting stronger covert articulation or more abstract semantic decisions—is needed to separate these alternatives. In addition, future studies could use tasks targeting specific contrasts related to semantic processing, auditory and motor aspects of language, and then establish the links between specific distance representations and these different effects.

One potential limitation of our work stems from our use of group-level brain parcellation methods to examine functional relationships with distance. This approach was pragmatic because it allowed us to look at whole-brain relationships without the high computational demands of examining individual vertices; however, it reduced the spatial resolution of our analysis, making it necessary to consider the extent to which spatial smoothing could account for any of the effects we report. We used the multimodal parcellation approach of Glasser et al. (2016) since this method improves subject to subject registrations and reduces inter-subject variability, which would add noise to our individual differences analysis (Coalson et al. 2018). It has been shown that these parcellated maps are highly stable across individual subjects: the mean pairwise Spearman rank correlation between subjects' individual maps was 0.94 for the T1w/T2w map (Burt et al. 2018). An alternative approach to our group-level parcellation approach would be to examine anatomical and functional variability within individuals to generate individual-specific areal-level parcellations to examine the relationship between brain function and physical distance.

Many of the functional effects we found to be associated with distance from sensory-motor landmarks cannot be readily explained in terms of loss of spatial resolution or smoothing. We used 2 mm surface-based smoothing to reduce the vertex-wise noise, to increase the statistical power to detect effects, and to satisfy statistical assumptions (i.e. the normal error distribution). Coalson et al. (2018) systematically explored the effects of spatial smoothing in the volume and on the surface. They found that surface-based smoothing does not blur across sulci or across tissue categories: even for 4 mm surface-based smoothing, parcels such as 55b and primary motor cortex are still distinct using intrinsic connectivity, myelin, language task activation, and a mean curvature map illustrating the folding pattern (Coalson et al. 2018; Glasser et al. 2016). Based on these results, we can be confident that effects for 55b cannot be explained in terms of blurred effects of motor activation (for example, variation in the size of motor cortex). Distance relationships in pIFS and 47m, which are located further from sensory-motor cortex, are even less likely to be explained in terms of spatial smoothing. This concern seems to be greatest for parcels in and around primary auditory cortex, where we found more activation for spoken language inputs with less distance between A1/TA2 and the temporal transverse sulcus; for these areas, it may be difficult to fully discount the possibility that distance relationships do not result from more activation within the sulcus itself. Nevertheless, the broader linear association we observed between principal gradient values and the correlation between distance and activation across many parcels seems unlikely to be explained in terms of localization issues relating to spatial smoothing or parcellation.

The unique contribution of our study is to provide evidence that the language functions of cortical regions are related to their physical distance to sensory-motor cortex. This study uses language as a domain in which to explore the diverse functional consequences of geodesic distance from sensory-motor landmarks within areas proximal to transmodal and unimodal cortex. Future studies can establish whether these principals of brain organization are universal, extending to other cognitive domains that also involve the recruitment of both transmodal and unimodal regions.

Supplementary Material

Supplementary material is available at *Cerebral Cortex* online.

Funding

The research was funded by a European Research Council Consolidator grant (Project ID: 771863—FLEXSEM) to E.J., by Scientific Foundation of Institute of Psychology, Chinese Academy of Sciences Grant (Grant number E1CX4725CX) , the National High-end Foreign Experts Recruitment Plan (Grant number G2022055007L), and Shandong Social Science Planning Fund Program (youth project, Grant number 20DYYJ04) to X.W., and by the National Key Research and Development Program of China (Grant number 2021ZD0201501), the National Natural Science Foundation of China (Grant number 31822024) and the Strategic Priority Research Program of Chinese Academy of Sciences (Grant number XDB32010300), and Scientific Foundation of Institute of Psychology, Chinese Academy of Sciences (Grant number E2CX3625CX) to Y.D..

Conflict of interest statement: None declared.

Author Contributions

X.W., B.C.B., D.S.M., J.S., and E.J. designed the research; X.W. analyzed data; K.K.R., M.Z., Z.C., X.W., and T. K. provided suggestions about data analysis; X.W. and E.J. wrote the original manuscript. All authors edited the manuscript.

References

Albouy P, Benjamin L, Morillon B, Zatorre RJ. Distinct sensitivity to spectrotemporal modulation supports brain asymmetry for speech and melody. *Science*. 2020:1979(367):1043–1047. https://doi.org/10.1126/science.aaz3468.

Andrews-Hanna JR, Reidler JS, Sepulcre J, Poulin R, Buckner RL. Functional-anatomic fractionation of the brain's default network. *Neuron*. 2010:25;65(4):550–62.

Badre D, D'Esposito M. Functional magnetic resonance imaging evidence for a hierarchical organization of the prefrontal cortex. *J Cogn Neurosci*. 2007:19(12):2082–2099. https://doi.org/10.1162/jocn.2007.19.12.2082.

Badre D, Nee DE. Frontal Cortex and the Hierarchical Control of Behavior. *Trends Cogn Sci*. 2018:22(2):170–188. https://doi.org/10.1016/j.tics.2017.11.005.

Badre D, Hoffman J, Cooney JW, D'Esposito M. Hierarchical cognitive control deficits following damage to the human frontal lobe. *Nat Neurosci*. 2009:12(4):515–522. https://doi.org/10.1038/nn.2277.

Barch DM, Burgess GC, Harms MP, Petersen SE, Schlaggar BL, Corbetta M, Glasser MF, Curtiss S, Dixit S, Feldt C, et al. Function in the human connectome: Task-fMRI and individual differences in behavior. *NeuroImage*. 2013:80:169–189. https://doi.org/10.1016/j.neuroimage.2013.05.033.

Benjamini Y, Hochberg Y. Controlling the false discovery rate: a practical and powerful approach to multiple testing. *Journal of the Royal statistical society: series B (Methodological)*. 1995:57(1):289–300.

Bi Y. Dual coding of knowledge in the human brain. *Trends Cogn Sci*. 2021:25(10):883–895. https://doi.org/10.1016/j.tics.2021.07.006.

Binder JR, Desai RH. The neurobiology of semantic memory. *Trends Cogn Sci*. 2011:15(11):527–536. https://doi.org/10.1016/J.TICS.2011.10.001.

Binder JR, Gross WL, Allendorfer JB, Bonilha L, Chapin J, Edwards JC, Grabowski TJ, Langfitt JT, Loring DW, Lowe MJ, et al. Mapping anterior temporal lobe language areas with fMRI: A multicenter normative study. *NeuroImage*. 2011:54(2):1465–1475. https://doi.org/10.1016/J.NEUROIMAGE.2010.09.048.

Bonner MF, Peelle JE, Cook PA, Grossman M. Heteromodal conceptual processing in the angular gyrus. *NeuroImage*. 2013:71:175–186. https://doi.org/10.1016/j.neuroimage.2013.01.006.

Braga RM, DiNicola LM, Becker HC, Buckner RL. Situating the left-lateralized language network in the broader organization of multiple specialized large-scale distributed networks. *J Neurophysiol*. 2020:124(5):1415–1448. https://doi.org/10.1152/JN.00753.2019.

Buckner RL, DiNicola LM. The brain's default network: updated anatomy, physiology and evolving insights. *Nat Rev Neurosci*. 2019, 201920:10:20:593–608. https://doi.org/10.1038/s41583-019-0212-7.

Buckner RL, Krienen FM. The evolution of distributed association networks in the human brain. *Trends Cogn Sci*. 2013:17(12):648–665. https://doi.org/10.1016/j.tics.2013.09.017.

Buckner RL, Margulies DS. Macroscale cortical organization and a default-like apex transmodal network in the marmoset monkey. *Nat Commun*. 2019:10(1):1976. https://doi.org/10.1038/s41467-019-09812-8.

Burt JB, Demirtaş M, Eckner WJ, Navejar NM, Ji JL, Martin WJ, Bernacchia A, Anticevic A, Murray JD. Hierarchy of transcriptomic specialization across human cortex captured by structural neuroimaging topography. *Nat Neurosci*. 2018:21(9):1251–1259. https://doi.org/10.1038/s41593-018-0195-0.

Burt JB, Helmer M, Shinn M, Anticevic A, Murray JD. Generative modeling of brain maps with spatial autocorrelation. *NeuroImage*. 2020:220:117038. https://doi.org/10.1016/j.neuroimage.2020.117038.

Chang EF, Kurteff G, Andrews JP, Briggs RG, Conner AK, Battiste JD, Sughrue ME. Pure apraxia of speech after resection based in the posterior middle frontal gyrus. *Neurosurgery*. 2020:87(3):E383–E389. https://doi.org/10.1093/neuros/nyaa002.

Chaudhuri R, Knoblauch K, Gariel MA, Kennedy H, Wang XJ. A large-scale circuit mechanism for hierarchical dynamical processing in the primate cortex. *Neuron*. 2015:88(2):419–431. https://doi.org/10.1016/j.neuron.2015.09.008.

Chevillet M, Riesenhuber M, Rauschecker JP. Functional correlates of the anterolateral processing hierarchy in human auditory cortex. *J Neurosci*. 2011:31(25):9345–9352. https://doi.org/10.1523/JNEUROSCI.1448-11.2011.

Chiou R, Humphreys GF, Jung JY, Lambon Ralph MA. Controlled semantic cognition relies upon dynamic and flexible interactions between the executive 'semantic control' and hub-and-spoke 'semantic representation' systems. *Cortex*. 2018:103:100–116. https://doi.org/10.1016/j.cortex.2018.02.018.

Coalson TS, van Essen DC, Glasser MF. The impact of traditional neuroimaging methods on the spatial localization of cortical areas. *Proc Natl Acad Sci U S A*. 2018:115(27):E6356–E6365. https://doi.org/10.1073/pnas.1801582115.

Connolly AC, Gobbini MI, Haxby JV. Three virtues of similarity-based multivariate pattern analysis: an example from the human object vision pathway. In: Visual population codes: toward a common multivariate framework for cellrecording and functional imaging (Kriegeskorte N, Kreiman G, eds). Cambridge, MA: MIT. https://doi.org/10.7551/mitpress/8404.003.0016.

Coutanche MN, Thompson-Schill SL. Creating concepts from converging features in human cortex. *Cereb Cortex*. 2015:25(9):2584–2593. https://doi.org/10.1093/cercor/bhu057.

Dale AM, Fischl B, Sereno MI. Cortical surface-based analysis: I. segmentation and surface reconstruction. *NeuroImage*. 1999:9(2):179–194. https://doi.org/10.1006/nimg.1998.0395.

Davis MH, Johnsrude IS. Hierarchical processing in spoken language comprehension. *J Neurosci*. 2003:23(8):3423–3431. https://doi.org/10.1523/JNEUROSCI.23-08-03423.2003.

Desikan RS, Ségonne F, Fischl B, Quinn BT, Dickerson BC, Blacker D, Buckner RL, Dale AM, Maguire RP, Hyman BT, et al. An automated labeling system for subdividing the human cerebral cortex on MRI scans into gyral based regions of interest. *NeuroImage*. 2006:31(3):968–980. https://doi.org/10.1016/j.neuroimage.2006.01.021.

Destrieux C, Fischl B, Dale A, Halgren E. Automatic parcellation of human cortical gyri and sulci using standard anatomical nomenclature. *NeuroImage*. 2010:53(1):1–15. https://doi.org/10.1016/j.neuroimage.2010.06.010.

Dichter BK, Breshears JD, Leonard MK, Chang EF. The control of vocal pitch in human laryngeal motor cortex. *Cell*. 2018:174(1):21–31.e9. https://doi.org/10.1016/J.CELL.2018.05.016.

Du Y, Buchsbaum BR, Grady CL, Alain C. Noise differentially impacts phoneme representations in the auditory and speech motor systems. *Proc Natl Acad Sci U S A*. 2014:111(19):7126–7131. https://doi.org/10.1073/pnas.1318738111.

Du Y, Buchsbaum BR, Grady CL, Alain C. Increased activity in frontal motor cortex compensates impaired speech perception in older adults. *Nat Commun*. 2016:7(1):1–12. https://doi.org/10.1038/ncomms12241.

Fedorenko E, Behr MK, Kanwisher N. Functional specificity for high-level linguistic processing in the human brain. *Proc Natl Acad Sci*. 2011:108(39):16428–16433. https://doi.org/10.1073/pnas.1112937108.

Fedorenko E, Hsieh PJ, Nieto-Castañón A, Whitfield-Gabrieli S, Kanwisher N. New method for fMRI investigations of language: defining ROIs functionally in individual subjects. *Journal of neurophysiology*. 2010:104(2):1177–94.

Felleman DJ, Van Essen DC. Distributed hierarchical processing in the primate cerebral cortex. *Cereb Cortex*. 1991:1(1):1–47. https://doi.org/10.1093%2Fcercor%2F1.1.1.

Fischl B, Sereno MI, Dale AM. Cortical surface-based analysis: II. Inflation, flattening, and a surface-based coordinate system. *NeuroImage*. 1999:9(2):195–207. https://doi.org/10.1006/nimg.1998.0396.

Fischl B, van der Kouwe A, Destrieux C, Halgren E, Ségonne F, Salat DH, Busa E, Seidman LJ, Goldstein J, Kennedy D, et al. Automatically parcellating the human cerebral cortex. *Cereb Cortex*. 2004:14(1):11–22. https://doi.org/10.1093/cercor/bhg087.

Glasser MF, Sotiropoulos SN, Wilson JA, Coalson TS, Fischl B, Andersson JL, Xu J, Jbabdi S, Webster M, Polimeni JR, et al. The minimal preprocessing pipelines for the Human Connectome Project. *NeuroImage*. 2013:80:105–124. https://doi.org/10.1016/j.neuroimage.2013.04.127.

Glasser MF, Coalson TS, Robinson EC, Hacker CD, Harwell J, Yacoub E, Ugurbil K, Andersson J, Beckmann CF, Jenkinson M, et al. A multi-modal parcellation of human cerebral cortex. *Nature*. 2016:536(7615):171–178. https://doi.org/10.1038/nature18933.

Grayson DS, Fair DA. Development of large-scale functional networks from birth to adulthood: A guide to the neuroimaging

literature. *NeuroImage*. 2017:160:15–31. https://doi.org/10.1016/j.neuroimage.2017.01.079.

Hamilton LS, Oganian Y, Hall J, Chang EF. Parallel and distributed encoding of speech across human auditory cortex. *Cell*. 2021:184(18):4626–4639.e13. https://doi.org/10.1016/j.cell.2021.07.019.

Hill J, Inder T, Neil J, Dierker D, Harwell J, Van ED. Similar patterns of cortical expansion during human development and evolution. *Proc Natl Acad Sci*. 2010:107(29):13135–13140. https://doi.org/10.1073/PNAS.1001229107.

Hoffman P, Binney RJ, Lambon Ralph MA. Differing contributions of inferior prefrontal and anterior temporal cortex to concrete and abstract conceptual knowledge. *Cortex*. 2015:63:250–266. https://doi.org/10.1016/j.cortex.2014.09.001.

Humphreys GF, Hoffman P, Visser M, Binney RJ, Lambon Ralph MA. Establishing task- and modality-dependent dissociations between the semantic and default mode networks. *Proc Natl Acad Sci U S A*. 2015:112(25):7857–7862. https://doi.org/10.1073/pnas.1422760112.

Huntenburg JM, Bazin PL, Margulies DS. Large-scale gradients in human cortical organization. *Trends Cogn Sci*. 2018:22(1):21–31. https://doi.org/10.1016/j.tics.2017.11.002.

Irish M, Hodges JR, Piguet O. Right anterior temporal lobe dysfunction underlies theory of mind impairments in semantic dementia. *Brain*. 2014:137(4):1241–1253. https://doi.org/10.1093/brain/awu003.

Jasmin K, Lima CF, Scott SK. Understanding rostral–caudal auditory cortex contributions to auditory perception. *Nat Rev Neurosci*. 2019:20(7):425–434. https://doi.org/10.1038/s41583-019-0160-2.

Ji JL, Spronk M, Kulkarni K, Repovš G, Anticevic A, Cole MW. Mapping the human brain's cortical-subcortical functional network organization. *NeuroImage*. 2019:185:35–57. https://doi.org/10.1016/j.neuroimage.2018.10.006.

Jones EG, Powell TPS. An anatomical study of converging sensory pathways. *Brain*. 1970:xci:793–820.

Koechlin E, Ody C, Kouneiher F. The architecture of cognitive control in the human prefrontal cortex. *Science*. 2003:1979(302):1181–1185. https://doi.org/10.1126/science.1088545.

Lipkin B, Tuckute G, Affourtit J, Small H, Mineroff Z, Kean H, Jouravlev O, Rakocevic L, Pritchett B, Siegelman M, et al. LanA (Language Atlas): A probabilistic atlas for the language network based on fMRI data from >800 individuals. *bioRxiv*. 2022. https://doi.org/10.1101/2022.03.06.483177.

Margulies DS, Ghosh SS, Goulas A, Falkiewicz M, Huntenburg JM, Langs G, Bezgin G, Eickhoff SB, Castellanos FX, Petrides M, et al. Situating the default-mode network along a principal gradient of macroscale cortical organization. *Proc Natl Acad Sci*. 2016:113(44):12574–12579. https://doi.org/10.1073/pnas.1608282113.

Mckeown B, Strawson WH, Wang H-T, Karapanagiotidis T, Vos de Wael R, Benkarim O, Turnbull A, Margulies D, Jefferies E, McCall C, et al. The relationship between individual variation in macroscale functional gradients and distinct aspects of ongoing thought. *NeuroImage*. 2020:220:117072. https://doi.org/10.1016/j.neuroimage.2020.117072.

Mesulam M-M. From sensation to cognition. *Brain*. 1998:121(6):1013–1052.

Mitchell JSB, Mount DM, Papadimitriou CH. Discrete geodesic problem. *SIAM J Comput*. 1987:16(4):647–668. https://doi.org/10.1137/0216045.

Muret D, Root V, Kieliba P, Clode D, Makin TR. Beyond body maps: Information content of specific body parts is distributed across the somatosensory homunculus. *Cell Rep*. 2022:38(11):110523. https://doi.org/10.1016/j.celrep.2022.110523.

Murphy C, Jefferies E, Rueschemeyer SA, Sormaz M, Ting WH, Margulies DS, Smallwood J. Distant from input: Evidence of regions within the default mode network supporting perceptually-decoupled and conceptually-guided cognition. *NeuroImage*. 2018:171:393–401. https://doi.org/10.1016/J.NEUROIMAGE.2018.01.017.

O'Rourke J. Computational geometry column 35. *ACM SIGACT News*. 1999:30(2):31–32. https://doi.org/10.1145/568547.568559.

Plaut DC. Graded modality-specific specialisation in semantics: A computational account of optic aphasia. *Cogn Neuropsychol*. 2002:19(7):603–639. https://doi.org/10.1080/02643290244000112.

Poologaindran A, Lowe SR, Sughrue ME. The cortical organization of language: distilling human connectome insights for supratentorial neurosurgery. *J Neurosurg*. 2020:134(6):1959–1966. https://doi.org/10.3171/2020.5.JNS191281.

Price C, Thierry G, Griffiths T. Speech-specific auditory processing: where is it? *Trends Cogn Sci*. 2005:9(6):271–276. https://doi.org/10.1016/J.TICS.2005.03.009.

Pylkkänen L. The neural basis of combinatory syntax and semantics. *Science*. 2019:66:62–66.

Ralph MAL, Jefferies E, Patterson K, Rogers TT. The neural and computational bases of semantic cognition. *Nat Rev Neurosci*. 2017:18(1):42–55. https://doi.org/10.1038/nrn.2016.150.

Robinson EC, Jbabdi S, Glasser MF, Andersson J, Burgess GC, Harms MP, Smith SM, Van Essen DC, Jenkinson M. MSM: A new flexible framework for Multimodal Surface Matching. *NeuroImage*. 2014:100:414–426. https://doi.org/10.1016/J.NEUROIMAGE.2014.05.069.

Sarubbo S, Tate M, de Benedictis A, Merler S, Moritz-Gasser S, Herbet G, Duffau H. Mapping critical cortical hubs and white matter pathways by direct electrical stimulation: an original functional atlas of the human brain. *NeuroImage*. 2020:205:116237. https://doi.org/10.1016/j.neuroimage.2019.116237.

Shaw SR, El-Omar H, Roquet D, Hodges JR, Piguet O, Ahmed RM, Whitton AE, Irish M. Uncovering the prevalence and neural substrates of anhedonia in frontotemporal dementia. *Brain*. 2021:144(5):1551–1564. https://doi.org/10.1093/brain/awab032.

Smallwood J, Bernhardt BC, Leech R, Bzdok D, Jefferies E, Margulies DS. The default mode network in cognition: a topographical perspective. *Nat Rev Neurosci*. 2021:22(8):503–513. https://doi.org/10.1038/s41583-021-00474-4.

Van Essen DC, Donahue CJ, Coalson TS, Kennedy H, Hayashi T, Glasser MF. Cerebral cortical folding, parcellation, and connectivity in humans, nonhuman primates, and mice. *Proc Natl Acad Sci U S A*. 2019:116(52):26173–26180. https://doi.org/10.1073/pnas.1902299116.

Visser M, Jefferies E, Embleton KV, Lambon Ralph MA. Both the middle temporal gyrus and the ventral anterior temporal area are crucial for multimodal semantic processing: distortion-corrected fmri evidence for a double gradient of information convergence in the temporal lobes. *J Cogn Neurosci*. 2012:24(8):1766–1778. https://doi.org/10.1162/jocn_a_00244.

Vos de Wael R, Benkarim O, Paquola C, Lariviere S, Royer J, Tavakol S, Xu T, Hong SJ, Langs G, Valk S, et al. Brain Space: a toolbox for the analysis of macroscale gradients in neuroimaging and connectomics datasets. *Communications Biology*. 2020:3(1):1–10. https://doi.org/10.1038/s42003-020-0794-7.

Wang X, Gao Z, Smallwood J. Both default and multiple-demand regions represent semantic goal information. *Journal of Neuroscience*. 2021:41:3679–3691.

Wen T, Duncan J, Mitchell DJ. Hierarchical representation of multistep tasks in multiple-demand and default mode networks. *J Neurosci*. 2020:40(40):7724–7738. https://doi.org/10.1523/JNEUROSCI.0594-20.2020.

Wang X, Men W, Gao J, Caramazza A, Bi Y. Two forms of knowledge representations in the human brain. *Neuron*. 2020a:107(2): 383–393.e5. https://doi.org/10.1016/j.neuron.2020.04.010.

Wang X, Margulies DS, Smallwood J, Jefferies E. A gradient from long-term memory to novel cognition: transitions through default mode and executive cortex. *NeuroImage*. 2020b:117074:1–12. https://doi.org/10.1016/j.neuroimage.2020.117074.

Woolrich MW, Ripley BD, Brady M, Smith SM.Temporal autocorrelation in univariate linear modeling of FMRI data.*Neuroimage*. 2001:1;14(6):1370–86.

Xu T, Nenning KH, Schwartz E, Hong SJ, Vogelstein JT, Goulas A, Fair DA, Schroeder CE, Margulies DS, Smallwood J, et al. Cross-species functional alignment reveals evolutionary hierarchy within the connectome. *NeuroImage*. 2020:223:117346. https://doi.org/10.1016/j.neuroimage.2020.117346.

Zhao Y, Song L, Ding J, Lin N, Wang Q, Du X, Sun R, Han Z. Left anterior temporal lobe and bilateral anterior cingulate cortex are semantic hub regions: Evidence from behavior-nodal degree mapping in brain-damaged patients. *J Neurosci*. 2017:37(1): 141–151. https://doi.org/10.1523/JNEUROSCI.1946-16.2016.